IOSR Journal of Electronics and Communication Engineering (IOSR-JECE)
e-ISSN: 2278-2834,p- ISSN: 2278-8735.Volume 13, Issue 1, Ver. I (Jan.- Feb. 2018), PP 75-98
www.iosrjournals.org

Multiple/Distributed Target Detection for HRR Signal Design

Mohammed Moazzam Moinuddin
Associate Professor, Dept. of ECE, Maulana Azad National Urdu University Polytechnic, Bangalore

Abstract— *For Multiple or Extended/Distributed targets such as background reflectors, the range sidelobes mask and corrupt observations of weak signals occurring near areas of strong returns. Therefore, sidelobe suppression is extremely important in precisely determining the echo scattering region. The notion of poly-semantic radar, which gave improved performance through coincidence detection, is analyzed for high resolution radar system in presence of high density additive noise and Doppler shift. These sequences are optimized by employing Hamming backtrack algorithm (HBT). The detection capability of poly-semantic sequences is further improved through coincidence detection of the return signal. A simulation procedure has been developed to accurately describe the signal returns from distributed targets, with pulse compression waveform coding.*

Keywords— *Sidelobe suppression, Extended/Distributed target, Range Resolution*

I. INTRODUCTION

In high resolution radar (HRR) systems, there is a need to employ sequences of larger lengths to achieve high pulse compression ratios [1], [2]. The Optimal binary codes (OBC) including Barker code (B13) and Golay codes [3] provide significant advantages in terms of detection and sidelobe suppression [4], but these codes are available at lower lengths less than 60. Earlier the generation of optimal sequences at higher length up to 5000 is developed for poly-alphabetic and bi-alphabetic sequences [5]-[7]. In poly-alphabetic radar [5] what is transmitted is a specially designed binary sequence so that there is no change in the transmission technology. On reception, it is decoded before further processing. This is a change in the current practice, the resistance to which has weakened, as decoding before further processing is also required by neural network processing [8]-[10] of radar return signal for additional advantage. After decoding, the return signal is subjected to multiple interpretations. Here, a binary sequence is transmitted, but through poly-gram reading, it can also be interpreted as quaternary and octal sequences. Thus, it is as if one sequence is physically transmitted, but three sequences are notionally transmitted and received. They can therefore be processed separately at the receiver to set up coincidence detection. In poly-alphabetic sequence design a bigram viewed as a quaternary element or a trigram viewed as an octal element is some what of a constrained concept. The Quaternary and octal elements as independent entities would have 3 and 7 first order Hamming neighbors, but bigrams and trigrams on the substratum of binary monograms, which undergo Hamming scan have only two and three first order Hamming neighbors. Thus, the higher order poly-gram interpretations have a disadvantage in Hamming scan. Also, the enlarged alphabets deteriorate the noise and Doppler robustness at higher lengths in poly-alphabetic sequence [6].

In order to overcome these drawbacks and to restrict the enlarged alphabets of poly- alphabetic sequence to binary, the poly-semantic sequences are proposed [11]. These sequences are mono-alphabetic nature of poly-alphabetic sequences. The work presented in [11] did not discuss about noise rejection ability of these sequences for detection a target in noise environment conditions. The work presented in this paper is an attempt to evaluate the detection ability of mono-alphabetic poly-semantic sequences for the application to high resolution radar in presence of high dense noise and Doppler frequency. In this paper, the detection performance of the detected signal in presence of additive noise and Doppler shift is evaluated in terms of figure of merit.
The figure of merit is defined [12] as,

$$F^{(m)} = \frac{\overline{C^{(m)}(0)} - \max\limits_{k\neq 0}\left[\overline{C^{(m)}(k)}\right]}{\overline{C^{(m)}(0)}} \qquad (1)$$

Here ‘m’ represents the number of bit errors obtained in the sequence. Thus, the figure of merit in (1) is defined in the context, when known number decoding errors are present in the detected signal. It is assume that

distortion due to propagation delay is ignored. Also, the additive noise is independent with transmitted signal. But, in real time situation, the received signal is corrupted by random noise with unknown noise strength. If the additive noise exceeds the threshold level (at the detector), the received sequence is not true replica of transmitted signal. The resulting signal at the output of the detector will undergo any number of bit errors. Then the optimal waveform design problem is solved by redefining the measure of performance in (1) by taking into the effect of additive random noise at given signal to noise ratio (η) as discussed in Sec. II.

II. DESIGN ALGORITHM AND ASSOCIATED CONCEPTS

The concept of mono-alphabetic poly-semanticism [11] is similar to adaptation of the self-cooperative sequences. A binary sequence S with good autocorrelation properties is designed. It is doubled in length by interleaving another binary sequence T_1 whose elements are so chosen that enlarged sequence is good. Yet another sequence T_2 is interleaved to triple the length and the elements of former are so chosen that the new enlarged T_3 sequence has good autocorrelation.

Let, $S=[S_0, S_1, S_2, \ldots, S_{N-1}]$ (2)

be a transmitted signal of length N,

$R=[R_0, R_1, R_2, \ldots, R_{N-1}]$ (3)

is received signal. Here, R = S + W; where W is the additive noise signal at given η.

Now, (1) is redefined as

$$F_\eta = \frac{\overline{C_\eta(0)} - \max_{k\neq 0}\left[\overline{C_\eta(k)}\right]}{\overline{C_\eta(0)}} \quad (4)$$

where, F_η is the figures of merit at given η.

The cross correlation between S & R at given η is

$$c_\eta(k) = \sum_{i=0}^{N-1-k} s_i r_{i+k},\ k = 0,1,2,\ldots,N-1 \quad (5)$$

Also, $F_\eta = 1 - \dfrac{\max_{k\neq 0}\left[\overline{C_\eta(k)}\right]}{\overline{C_\eta(0)}}$ or $F_\eta = 1 - \dfrac{1}{D_\eta}$ (6)

Where, $D_\eta = \dfrac{\overline{C_\eta(0)}}{\max_{k\neq 0}\left[\overline{C_\eta(k)}\right]}$ (7)

is the discrimination at given η.

The over head bars in (4) & (6) denote the averaging over the ensemble of R. The work presented in this paper considers the ensemble of R with 100 runs of additive noise signals in order to obtain more accurate performance. Here, F_η is a monotone function of D_η as in (6). When D_η goes to infinity, F_η becomes unity. The range of F_η is from 0 to 1, making F_η a non-euphuistic measure.

In the detection process by employing coincidence detection, the return signal R is triply processed to exploit the goodness at three different stages of construction. The criterion of goodness, which is used for design, takes into account the interaction of the three interleaved sequences T_1, T_2, and T_3.

Multiple Targets:

When there are N number of point targets (source of reflectors) clustered with in the sequence length period, the echos from the reflectors arrives at the receiver at different sub-pulse delays are added in the subsequent range bins. The resultant sequence length increases as the distance between two distinct targets increases. IF τ sec. is the sub-pulse duration, and N is the sequence length the maximum separation between the targets is Nτ sec. The no. of range cells required are (2N-1). Consider there are three targets separated at 2 τ and 5 τ respectively with first target. If B13 sequence is transmitted. The echo from these targets is given by

0 0 0 0 0 1 1 1 1 1 -1 -1 1 1 -1 -1 1 -1
0 0 0 1 1 1 1 1 -1 -1 1 1 -1 -1 1 -1
1 1 1 1 1 -1 -1 1 1 -1 -1 1 -1

The resultant is [1 1 1 2 2 2 2 3 2 1 1 2 -1 0 0 -2 1 -1]
The no. of range cells are 18.
Similarly we can add a maximum of N no. of sequences.

Distributed Targets:

The distributed targets such as clouds, thunderstorm, precipitation etc. for weather radar, consists of a number point scatterers, in which the target samples occupy more than the radar resolution cell. Therefore the echo sequences are added at every sub-pulse duration. i.e. If the distributed target has kτ sec duration, then k no. of sequences are added. For example if k=3, then

0 0 1 1 1 1 1 -1 -1 1 1 -1 -1 1 -1
0 1 1 1 1 1 -1 -1 1 1 -1 -1 1 -1
1 1 1 1 1 -1 -1 1 1 -1 -1 1 -1

The resultant sequence is [1 2 3 3 3 2 -1 -2 1 1 -1 -1
-1 0 -1].

Discrimination Factor and Figure of merit:

Since the matched filter output has multiple peaks corresponds to the multiple/ distributed targets. Discrimination Factor and Figure of merit can be defined as

Also, $$F_\eta^t = 1 - \frac{\max\limits_{k \neq [t]} \left[\overline{C_\eta(k)} \right]}{\overline{C_\eta(t)}} \quad \text{or} \quad F_\eta^t = 1 - \frac{1}{D_\eta^t} \qquad (8)$$

Where, $$D_\eta^t = \frac{\overline{C_\eta(t)}}{\max\limits_{k \neq [t]} \left[\overline{C_\eta(k)} \right]} \qquad (9)$$

Where t is an integer represents target position and [t] is an array of all target positions

A. Hamming backtrack algorithm for PSS

To optimize the performance of goodness, the poly-semantic sequences should undergo Hamming scan [5] by considering figure of merit as desideratum. The Hamming scan algorithm may not perform recursive search among all these Hamming neighbors and results in suboptimal solution to the signal design problem. When poly-semantic Hamming scan yields no sequence with a figure of merit better than the previous sequence, the backtracking Hamming scan algorithm can be employed to improve further the objective function of the resulting sequence. It considers a prescribed number n called span of the best Hamming neighbors (though they are all inferior to starting sequence) and improves them separately by repeated recursive Hamming scan, say c times (called climb). If some sequences superior to the starting poly-semantic sequence results, the best among them is selected. A span of 6 and a climb of 2 is used in the proposed algorithm. If the Hamming backtracking succeeds in improving the value of figure of merit, the search can resume by further application of poly-semantic Hamming scan.

B. Phase reversal effect due to Doppler shift

Another advantage of poly-semantic sequence arises because of its bi-phase mono-alphabetic nature. The bit error due to Doppler frequency occurs when the phase shift of the pulse exceeds $\pm\pi/2$ unlike the poly phase sequence which results into a bit error when phase shift exceeds $\pm\pi/M$, where M indicates the number of phase levels in the sequence. Fig. 1(a) shows the range of phase shift without bit errors for bi-phase sequences (M=2) and Fig. 1(b) for poly-phase sequences with M = 4.

In noise free environments, the phase shift added due to Doppler to the sub-pulses is monotonic function as required for goodness of measure. In poly-semantic sequences of length N, the maximum phase shift allowed on each sub-pulse of duration $\tau = T/N$ sec without bit errors is less than $\pm\pi/2N$. Where as in poly-phase sequences the maximum allowable phase shift is less than $\pm\pi/MN$ without bit errors. Therefore the poly-semantic sequences have M/2 times more Doppler tolerance when compared to poly phase sequences.

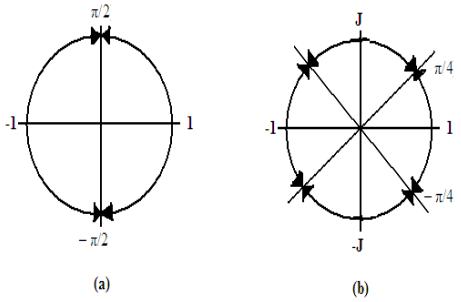

Fig. 1 Range of phase shift without bit errors (a) for bi-phase sequences (M=2) (b) poly-phase sequences with M = 4.

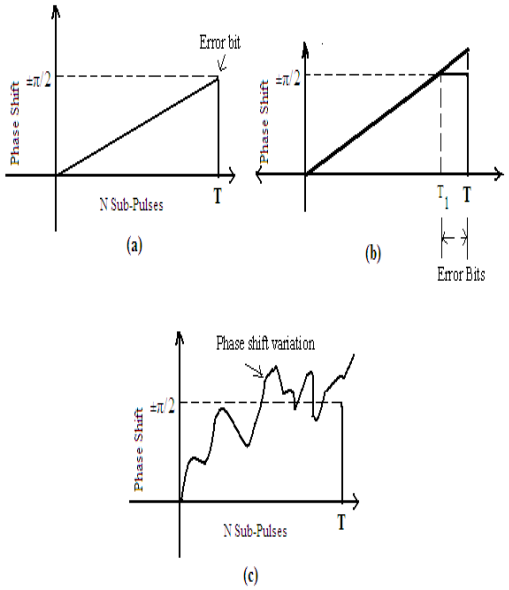

Fig. 2 Doppler phase shift on received bi-phase sequences (a) when phase shift is equal to $\pm\pi/2$ (b) when phase shift is greater than $\pm\pi/2$ (c) when additive noise is added along with Doppler phase shift.

In poly-semantic sequences, when the phase shift is equal to $\pm\pi/2$, the last sub-pulse in the sequence takes phase reversal. So the last bit produces an error as shown in Fig. 2 (a). When the phase shift exceeds $\pm\pi/2$, the bits within the period T_1 & T (where, $T_1<T$) in Fig. 2(b) results into an error.

III. POLY-SEMANTIC RADAR SIGNAL PROCESSOR

The generation of poly-semantic sequences is completed in two steps: first one using restricted (selective) Hamming backtracking scan for interspersed binary sequences and the second, using a complete Hamming backtracking scan with an appropriate joint objective function, which takes into the account of correlation properties between the sequence S and predefined interleaved sequences in the process of signal design. The block schematic diagram of poly-semantic radar signal processor at the transmitter is shown in Fig. 3(a).

A. First step in the signal design

Consider, optimal binary codes or randomly generated binary codes of length N, given by

$$S_1 = A = [a_j] \quad (10)$$

$$B = [b_j] \quad (11)$$

and $$C = [c_j] \quad (12)$$

Where, j = 0, 1 ,2, 3 , …, N-1.

The elements of these sequences are drawn from alphabet
{-1, +1}.

The sequence S_1 is mutated *viz.* +1 → -1, - 1→ +1 using Hamming backtracking scan algorithm to get optimum figure of merit. The sequences S_2 of length 2N and S_3 of length 3N are generated by interleaving the elements of S_1&B and S_2&C respectively as shown in Fig. 3(a). Therefore

$$S_2=[a_jb_j] \quad (13)$$

And $$S_3=[a_jb_jc_j] \quad (14)$$

Where, j= 0, 1 ,2, 3 , …, N-1.

A selective Hamming backtracking scan algorithm [10] is applied on the sequences S_2 and S_3 , so that the figure of merit of the output sequence is optimized. This algorithm performs mutations only on the embedded elements, *i.e.*, b_0, b_1, b_2, b_3 … of the sequence S_2, and c_0, c_1, c_2, c_3 … of the sequence S_3, without disturbing the other elements.

The sequence S_3 is interspersed by binary sequences S_1 and S_2. It is equivalent to three sequences with good autocorrelation properties being transmitted in the form of S_3.

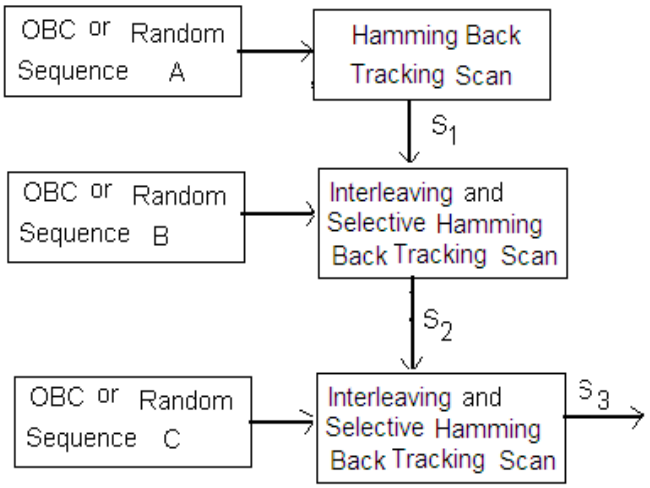

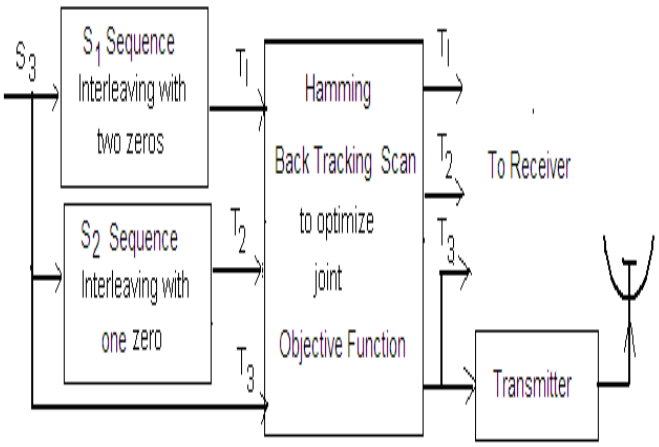

(a)

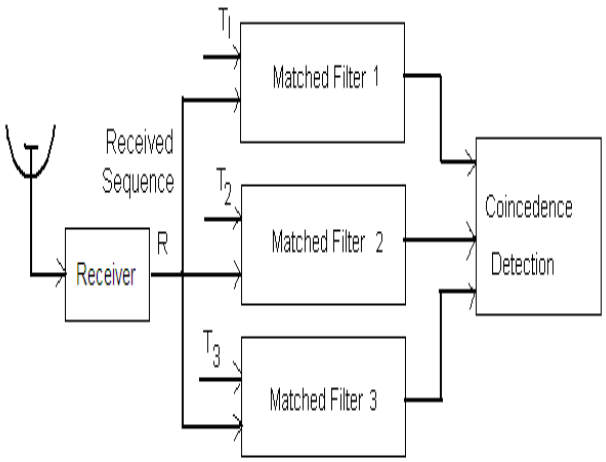

(b)

Fig. 3 Block schematic diagram of poly-semantic radar signal processor (a) Transmitter (b) Receiver.

B. Second step in the signal design

For further optimization, the following three sequences are derived from the sequence $S_3 = [a_j\ b_j\ c_j]$

$T_1 = [\ a_0, 0, 0,\ a_1, 0,\ 0,\ a_2, 0,\ 0\ \ldots\ a_{N-1}, 0, 0\ ]$ (15)
$T_2 = [\ a_0, b_0,\ 0,\ a_1,\ b_1,\ 0,\ a_2,\ b_2,\ 0\ \ldots a_{N-1},\ b_{N-1},\ 0\ ]$ (16)
$T_3 = [\ a_0, b_0, c_0, a_1,\ b_1,\ c_1,\ a_2, \ldots a_{N-1},\ b_{N-1},\ c_{N-1}\ ]$ (17)

These sequences T_1 and T_2 of length 3N are derived from the optimized sequences S_1 and S_2 embedded with zeros. The sequence T_3 is same as S_3.

The full Hamming scan algorithm is applied on the binary sequence S_3 and three derived sequences T_1, T_2 and T_3 for finding the pseudo-discriminations d_1, d_2 and d_3. The pseudo-discriminations d_1, d_2 and d_3 are defined on the basis of cross correlation of the sequences S_3 & T_1, S_3 & T_2 and S_3 & T_3 respectively. The pseudo-discrimination is the ratio of the peak when the sequences match lengthwise to the largest sidelobe amplitude in the cross correlation. The binary poly-semantic Hamming scan induces mutations in the elements of binary sequence S_3, *viz.*, +1 → -,1 - 1→ +1 and looks at the first order Hamming neighbors of all the elements in the sequence. A mutation in the element of S_3, in turn induces mutation in the corresponding elements of the sequences T_1, T_2 and T_3. The algorithm computes the sum (d) of pseudo-discriminations d_1, d_2 and d_3 (i.e $d = d_1+d_2+d_3$) of all the first order Hamming neighbors of S_3 and picks up the binary sequence which results in largest value of d. The autocorrelation due to each perturbation of the binary sequence is calculated by merely taking into account the changes required in the original autocorrelation instead of calculating the aperiodic

autocorrelation of the Hamming neighbors *ab initio*. This facilitates the expedition of the process of binary poly-semantic Hamming scan algorithm to obtain sequences of larger lengths.

the joint figure of merit $F = (F_1+F_2+F_3)/3$. Here, F_1, F_2, and F_3 are obtained from d_1,d_2, and d_3 respectively. The good figure of merit properties of these three interpretations are jointly used through coincidence detection for the detection of target. The binary sequence S_3 (T_3) is transmitted as a waveform.

The signal processing system at the receiver is shown in Fig. 3(b). On reception, the received waveform which is perturbed by Gaussian noise and / or Doppler shift is decoded into binary sequence (R). The received binary sequence R is cross correlated with three embedded sequences T_1, T_2, and T_3 (or S_3) in three channels separately. The three cross correlation peaks in three channels coincide, which simultaneously indicates the presence of the target (Fig. 9). It can also be observed that the time sidelobes in three channels do not align. This in turn reduces the degree of false alarm because of time sidelobes in the return signal.

IV. IMPROVED FIGURE OF MERIT OF PSS AT LARGER LENGTHS

The figure of merit of any sequence deteriorates as the noise strength increases and has individual performance deterioration pattern. That is the rate of deterioration can also vary from sequence to sequence. Thus, a sequence with superior performance at low noise levels could have a faster rate of deterioration than another sequence which has inferior performance at low noise levels compare with slower rate of deterioration. Under such situations, the ranking of sequences may be different at different noise levels [12], [13]. This situation becomes worse when the Doppler shift is also added to the return signal in addition to noise. But, for poly-semantic sequences the rate of deterioration in figure of merit remains uniform with respect to increase in noise and Doppler shift. The figure of merit of the poly-semantic sequence depends on the Hamming neighborhood of the transmitted signal so that the received signal is allowed to be anywhere in that neighborhood. Since the poly-semantic sequences are optimized with HBT algorithm, at higher sequence lengths (as the size of the neighborhood increases), it is possible to achieve better noise and Doppler performance in terms of figures of merit. Table I gives the figures of merit of poly-semantic sequences of length, N=39 to 6000. These results provide an evidence that the figure of merit is high at larger lengths and becomes stable as length increases.

TABLE I.
FIGURE OF MERIT AND DISCRIMINATION FOR
POLY-SEMANTIC SEQUENCES

length	d_1	d_2	d_3
39	1.85	4.33	7.8
75	2.083	4.54	9.37
150	3.125	4.76	11.53
180	3.157	5.21	12.0
270	4.28	7.2	14.21
300	4.166	9.09	15
360	5	8.57	15
450	5	9.37	16.07
600	6.06	8.510	17.64
750	5.81	10.63	17.85
1050	6.03	10.76	20.19
1500	7.81	10.63	22.05
2100	9.58	11.86	25
2400	9.63	14.03	26.08
2700	10	12.85	24.77
3000	10	17.39	27.02
3300	10.57	19.82	30.55
3900	11.50	14.94	28.26
4500	10.56	20.27	32.84
5100	12.5	20.35	32.48
6000	13.60	23.39	35.71

length	Fm_1	Fm_2	Fm_3	Fm
39	0.461	0.769	0.871	0.701
75	0.52	0.78	0.893	0.731
150	0.68	0.79	0.913	0.771
180	0.683	0.808	0.916	0.794
270	0.766	0.861	0.929	0.852
300	0.76	0.89	0.93	0.861
360	0.8	0.883	0.933	0.872
450	0.8	0.893	0.937	0.877
600	0.835	0.882	0.943	0.886
750	0.828	0.906	0.944	0.892
1050	0.834	0.907	0.950	0.897
1500	0.872	0.906	0.954	0.910
2100	0.895	0.915	0.96	0.924
2400	0.896	0.928	0.961	0.928
2700	0.9	0.9222	0.959	0.927
3000	0.9	0.942	0.963	0.935
3300	0.905	0.949	0.967	0.940
3900	0.913	0.933	0.964	0.936
4500	0.905	0.950	0.969	0.941
5100	0.92	0.950	0.969	0.946
6000	0.926	0.957	0.972	0.951

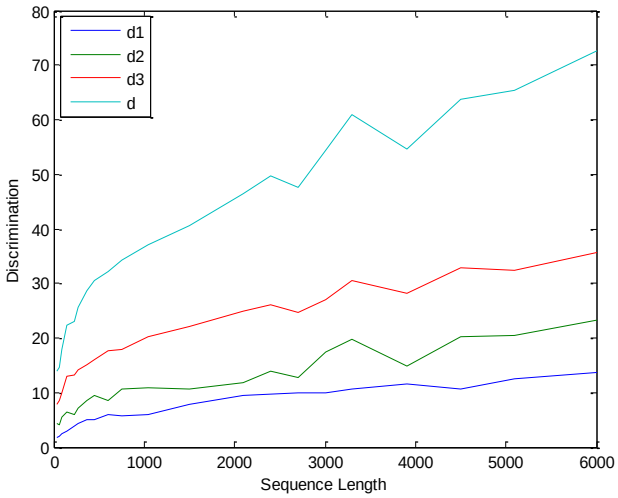

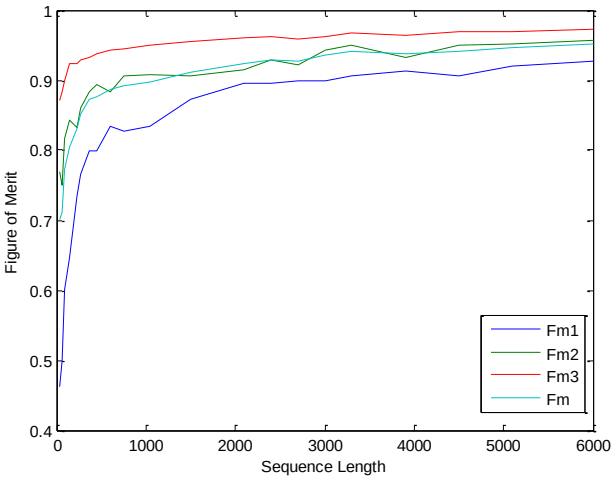

Fig. 4 discrimination and Figure of merit

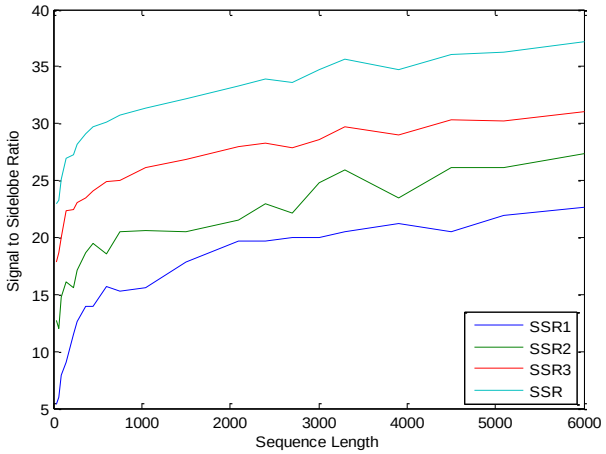

Fig. 5 Signal to sidelobe ratio

.

V. SIMULATION RESULTS AND PERFORMANCE EVALUTION

A. Noise robustness

When the PSS is perturbed by additive noise of different strengths, the noise effect on figures of merit and signal to noise ratio at different sequence lengths is shown in Fig. 6. The noise performance is examined for different values of η ranging between 10 dB to -10 dB. The noise performance results clearly show that the PSS exhibits high noise robustness at the higher sequence lengths.

B. Doppler tolerance

As explained in Sec. II, when the target has a constant motion, a linear phase shift given by $d\phi = \sigma\pi / N$, $0 < \sigma \leq 1$ proportional to target velocity will be added on to the received decoded sequence. The performance of poly-semantic sequences in terms of figure of merit and signal to noise ratio without additive noise is shown in the Fig. 7 at different Doppler phase shifts (φ_d) in the interval of [0.4π/N, 0.8π/N] per sub-pulse. It is observed from the figure that as Doppler shift increases above 0.5π/N, the performance of figure of merit deteriorates.

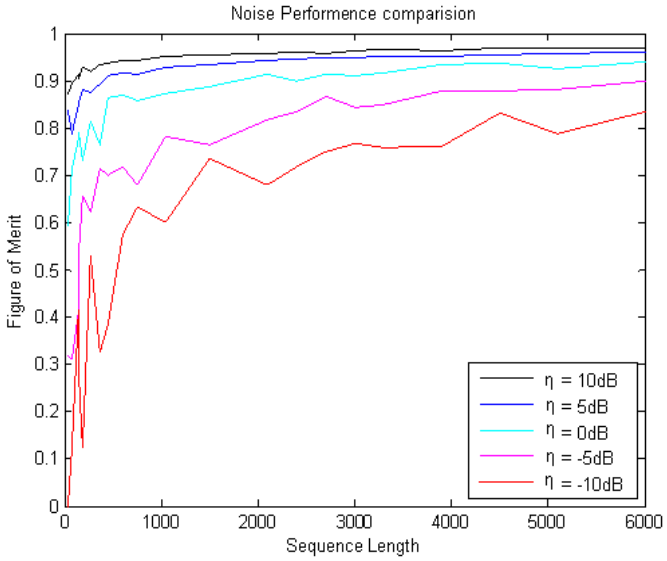

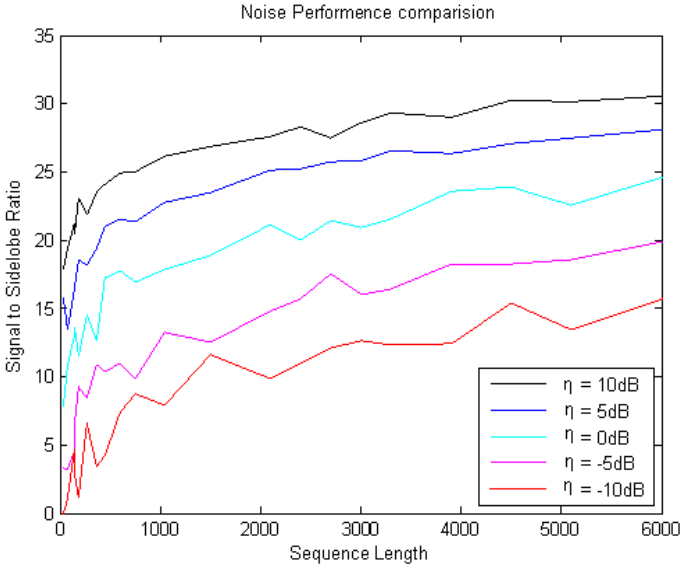

Fig. 6 Noise performance of poly-semantic sequences

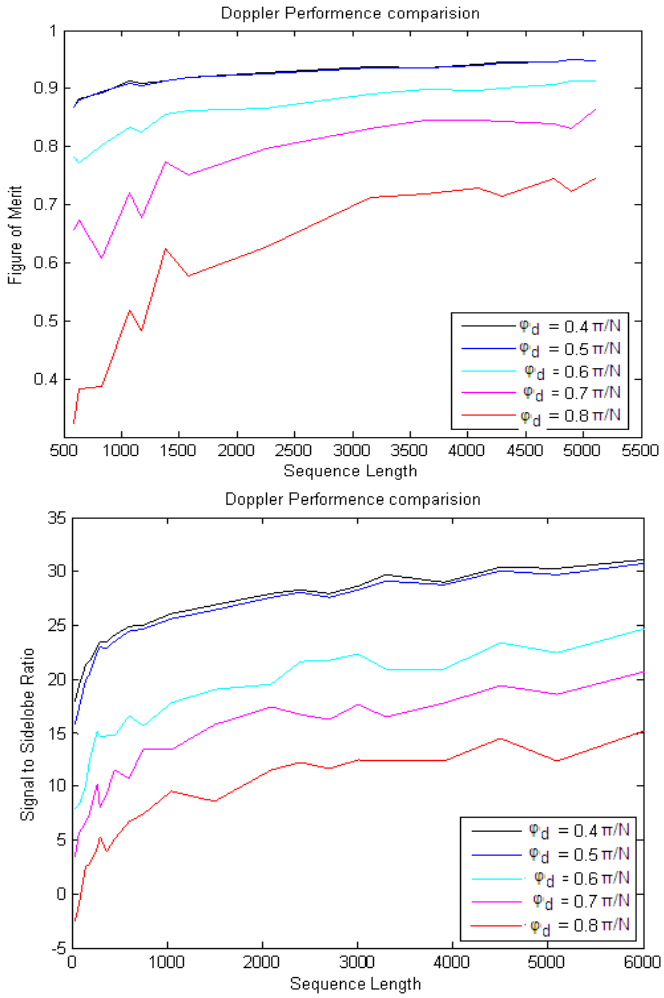

Fig. 7 Doppler performance of poly-semantic sequences

When Doppler phase shift increases to 0.8π/N, the figure of merit falls below 0.3 (Fig. 7). Thus the information due to target will be masked and it is not possible to identify the target. The proposed sequences have Doppler tolerance up to 0.7π/N with corresponding figure of merit of 0.3.

C. Combined effect of noise and Doppler shift

When the signal encounters the joint effect of additive noise and Doppler shift due to a moving target, the phase shift variation in the received signal becomes non-monotonic function as shown in Fig. 2(c). In such a case some of the sub-pulses (randomly) in the sequences may have phase shift more than $0.5\pi/N$. At threshold detection these sub-pulses undergo phase reversal. The performance of figure of merit decreases with the increase of such erroneous bits in the decoded sequence. This results into deterioration in the performance of PSS detection. Fig. 8 gives the figure of merit of PSS sequences at different lengths N=0 to 6000 at η = -5 dB and varying Doppler shift in the interval $[0.4\pi/N, 0.8\pi/N]$.

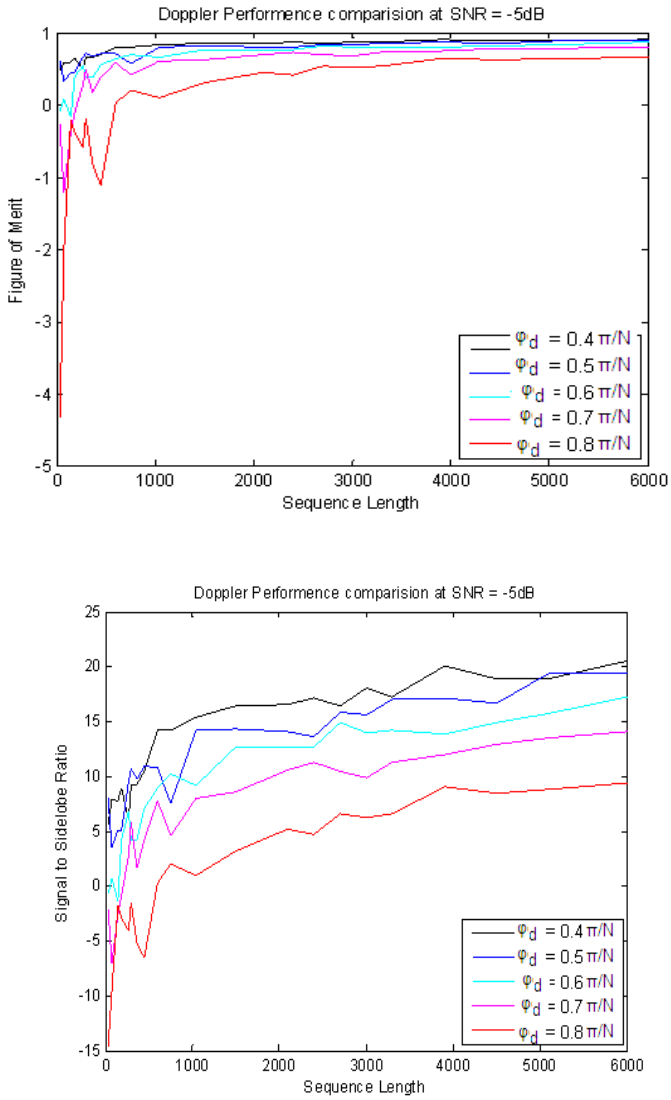

Fig. 8 Noise and Doppler performance of poly-semantic sequences at different Doppler phase shifts (φ_d) and fixed η of -5 dB.

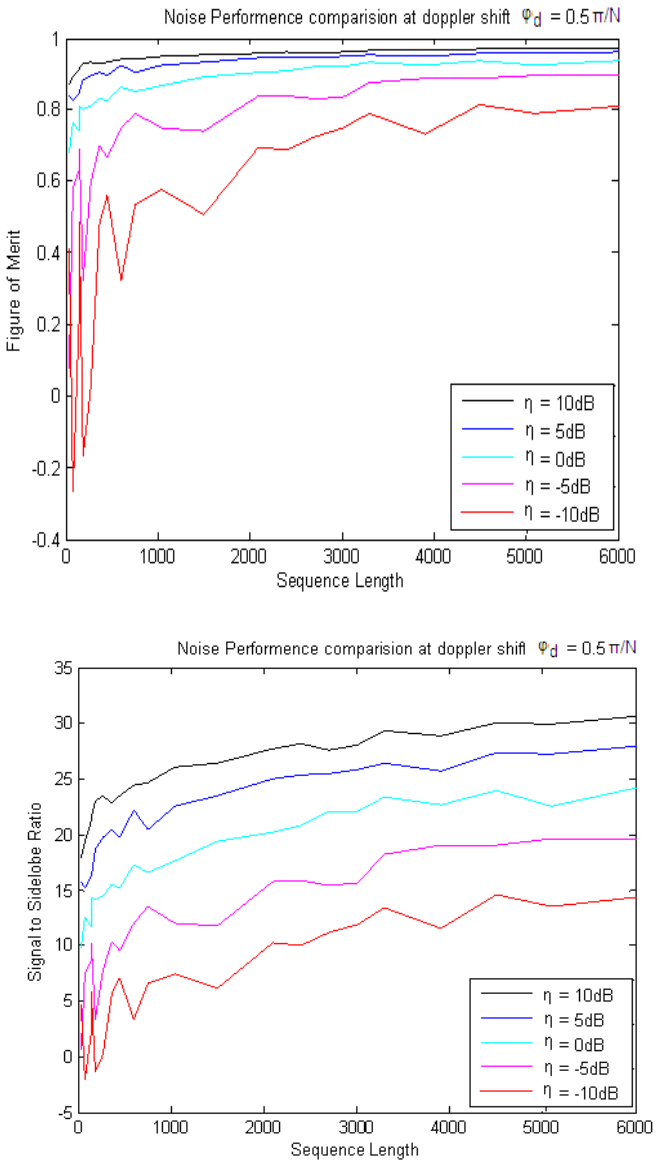

Fig. 9 Noise and Doppler performance of poly semantic sequences at different noise levels of η and fixed Doppler phase shift of 0.5π/N.

Also, Fig. 9 shows at fixed Doppler shift of 0.5π/N and varying η. It is observed that the sequences exhibits more Doppler tolerance at higher length when compared to lower length since the phase variation per bit is small at higher lengths.

D. Range Resolution

Consider the multiple/distributed targets, which are moving with within the resolution volume. Since the point reflectors are very close, assume that all are at same velocity. The following target model for N sources is developed with Doppler shift in noisy environment. This model is simulated using MATLAB functions. Also consider the targets, which are separated from different sub-pulses delay apart (SPDA) with sub-pulse duration 'τ' of 50 ns (range resolution 7.5 m). The sources are separated from one SPDA to a maximum of (N-1) SPDA. When targets are within the sub-pulse range, the resultant echo signal is the addition of all the echo signals from the targets. Depending on the delay between the echo signals, the length of the resultant sequence increases. Fig. 10 is designed as a simulated target model for generating received code S_R, when targets are at $n_1,n_2,n_3\ldots..n_N$ SPDA with Doppler phase shifts $\Phi_1, \Phi_2, \Phi_3,\ldots \Phi_N$ in noisy environment. The binary code S_b is clocked (2N-1) times into the target model to get the received code S_R of fixed length (2N-1). Limiter is used to limit the amplitude levels between ±1.

If $\Phi_1 = \Phi_2 = \Phi_3 \ldots = \Phi_N = \Phi$ the targets are at same velocity and if If $\Phi_1 = \Phi_2 = \Phi_3 \ldots = \Phi_N = 0$ all targets are stationary.

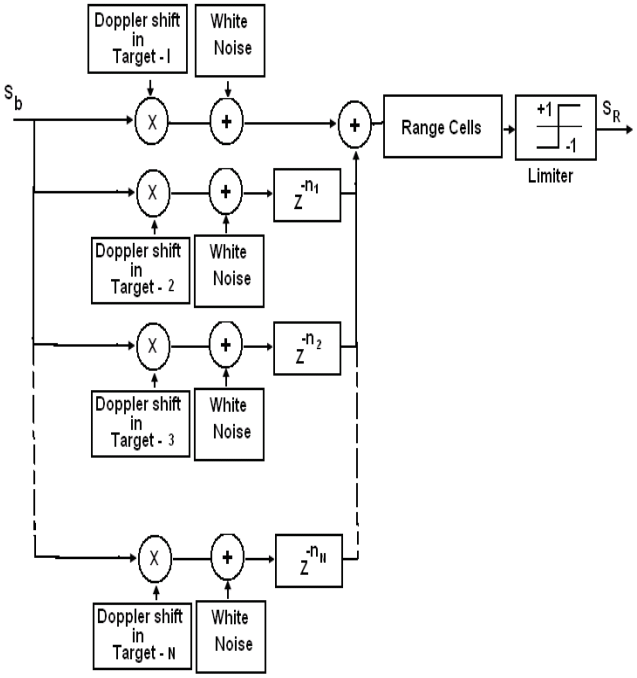

Fig. 10 Target model when N targets are at n- SPDA.

E. Detection Performance

Let us consider a K_a-band 30 GHz radar, transmitting a poly-semantic sequence of length N=1575 with pulse interval of 36.25 μs. The sub-pulse time interval τ is 50 ns (signal bandwidth is 20 MHz and range resolution is 7.5 m). At the receiver, the resultant waveform is multiply interpreted for coincidence detection.

For range resolution ability, consider a target model when a dispersed echo is reflected from two targets located at sub-pulse duration apart (SPDA) of zero to (N-1). Fig. 11 Shows Range Resolution ability between two targets (a) with no noise (b) at -5dB noise (c) Doppler shift=0.5 π /N When the targets are stationary, Fig. 12 (a) shows the output waveforms of poly-semantic sequences when two targets are at 50 SPDA in noise free environment, (b) when noise is at η = -10 dB. The targets can be detected even if the η falls to -15 dB as shown in Fig. 12(d).

Fig. 13 shows Poly-semantic sequences of length 3000 for (a) 10 targets at 2 SPDA (b) ten targets at 100 SPDA (c) 30 targets at 100 SPDA (d) 30 targets at 100 SPDA at -5dB noise (e) 100 targets at 30 SPDA at -5dB noise (f) 300 targets at 10 SPDA (g) 300 targets at 10 SPDA at -5dB noise (h) distributed target of duration 10 SPDA (i) distributed target of duration 20 SPDA (j) distributed target of duration 50 SPDA. This is not possible with conventional sequences.

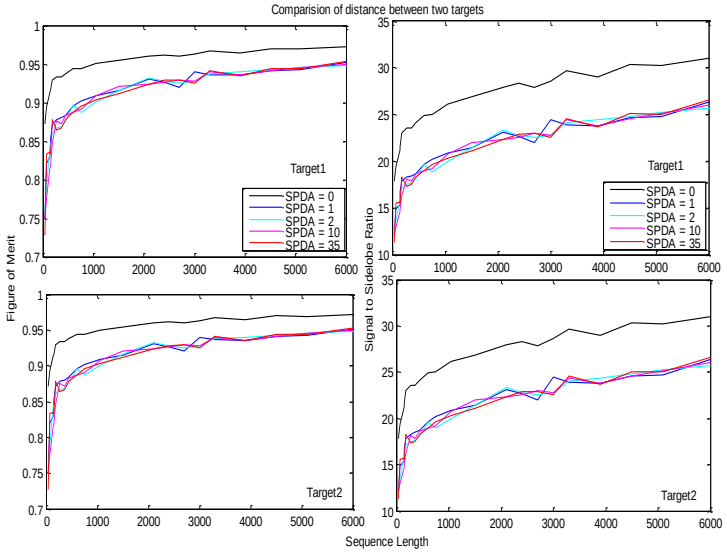
Comparision of distance between two targets
Figure of Merit
Signal to Sidelobe Ratio
Target1
Target2
SPDA = 0
SPDA = 1
SPDA = 2
SPDA = 10
SPDA = 35
Sequence Length

(a)

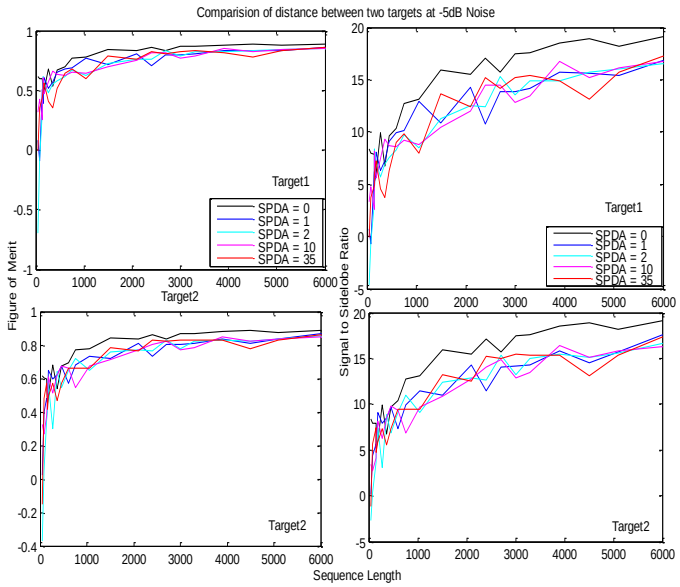
Comparision of distance between two targets at -5dB Noise
Figure of Merit
Signal to Sidelobe Ratio
Target1
Target2
SPDA = 0
SPDA = 1
SPDA = 2
SPDA = 10
SPDA = 35
Sequence Length

(b)

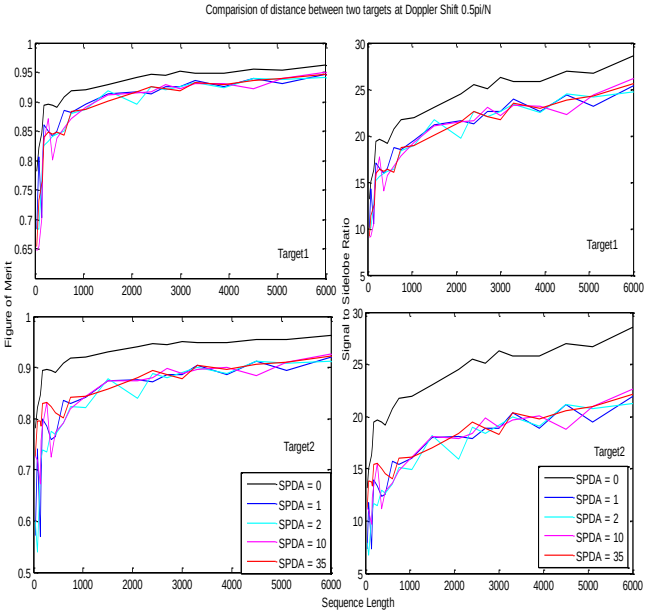

(c)

Fig. 11 Range Resolution ability between two targets (a) with no noise (b) at -5 dB noise (c)at Doppler shift =0.5 π /N

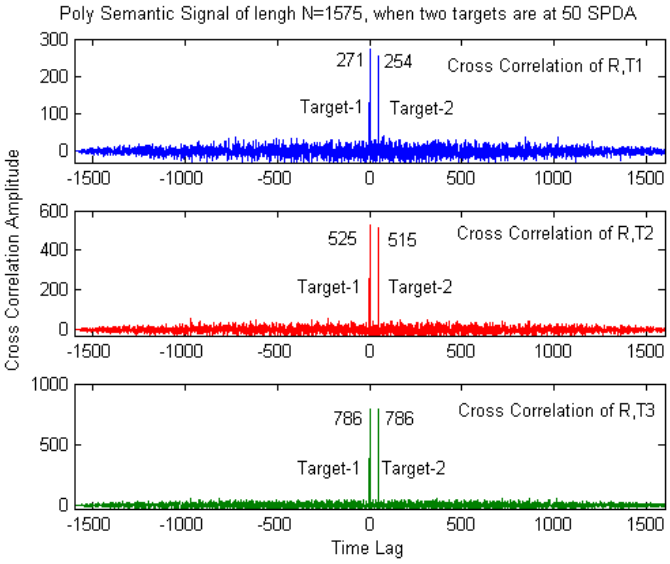

(a)

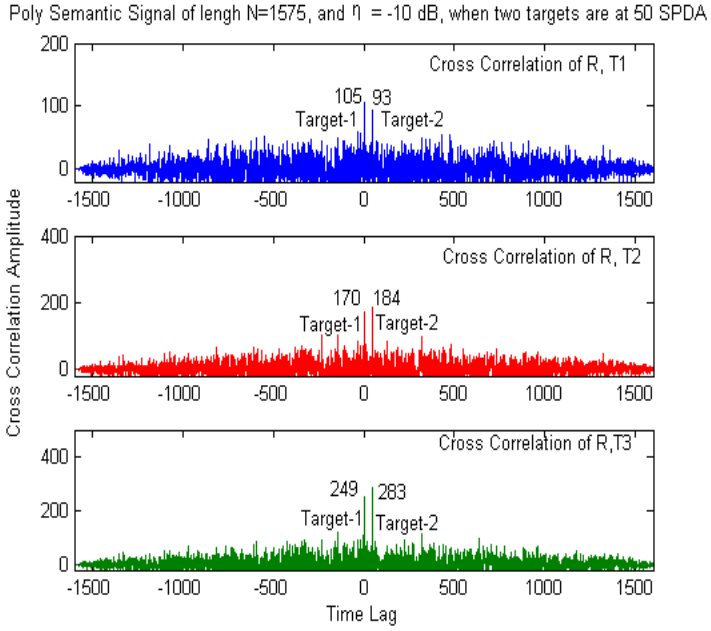
Poly Semantic Signal of lengh N=1575, and η = -10 dB, when two targets are at 50 SPDA
Cross Correlation of R, T1
105 93
Target-1
Target-2
Cross Correlation of R, T2
170 184
Target-1
Target-2
Cross Correlation of R,T3
249 283
Target-1
Target-2
Cross Correlation Amplitude
Time Lag

(b)

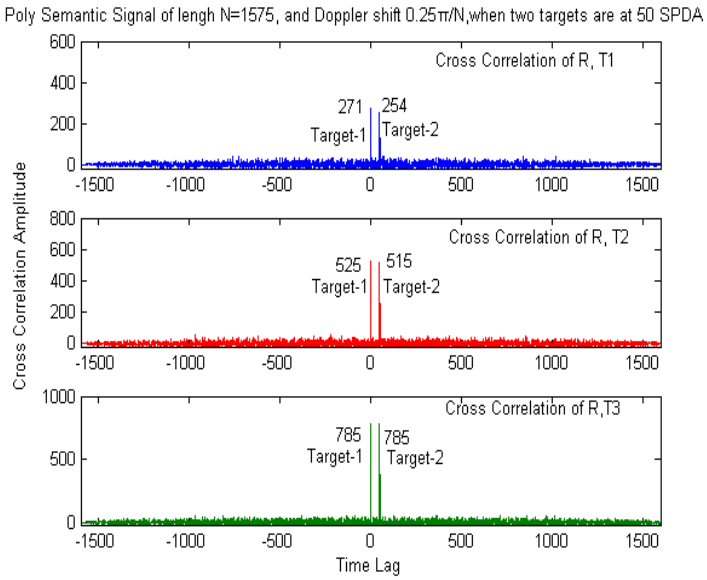
Poly Semantic Signal of lengh N=1575, and Doppler shift 0.25π/N,when two targets are at 50 SPDA
Cross Correlation of R, T1
271 254
Target-1
Target-2
Cross Correlation of R, T2
525 515
Target-1
Target-2
Cross Correlation of R,T3
785 785
Target-1
Target-2
Cross Correlation Amplitude
Time Lag

(c)

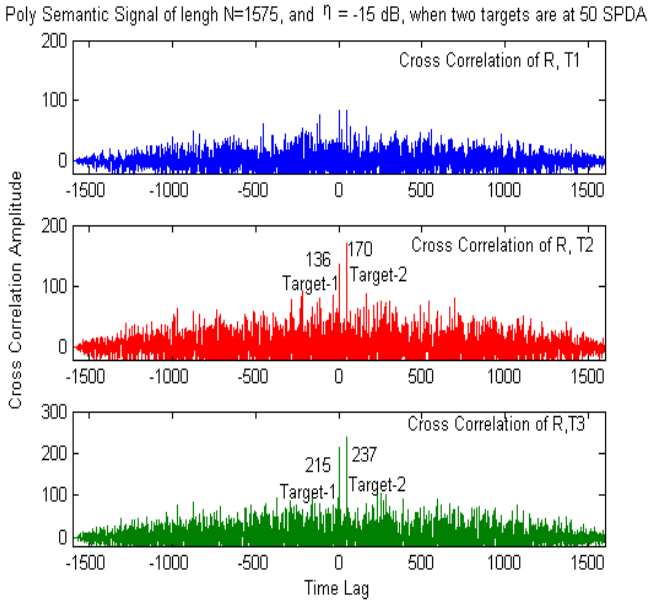

(d)

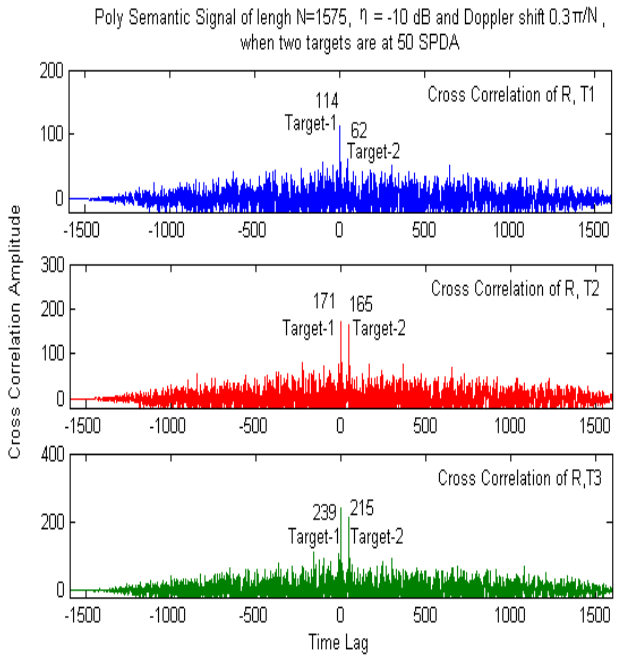

(e)

Fig. 12 Poly-semantic sequences of length 1575 for two targets at 50 SPDA (a) with no noise, (b) at η = -10 dB (c) at Doppler shift = 0.25π/N (d) at η =-15 dB and (e) at η =-10 dB and Doppler shift = 0.3π/N

Range resolution for more than two targets

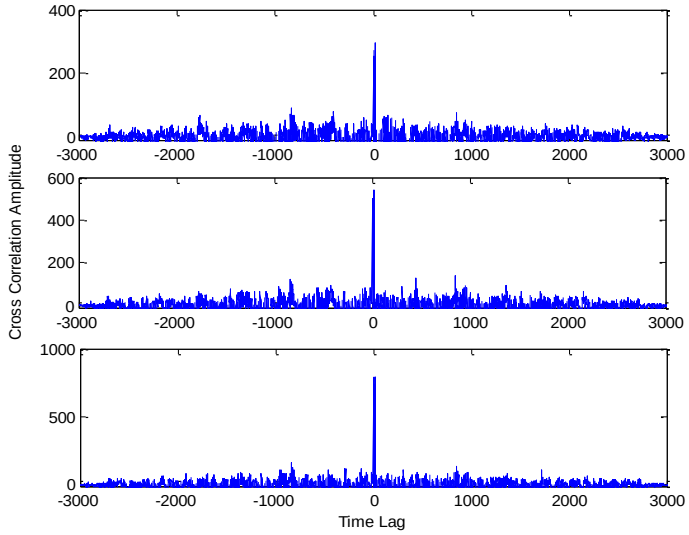

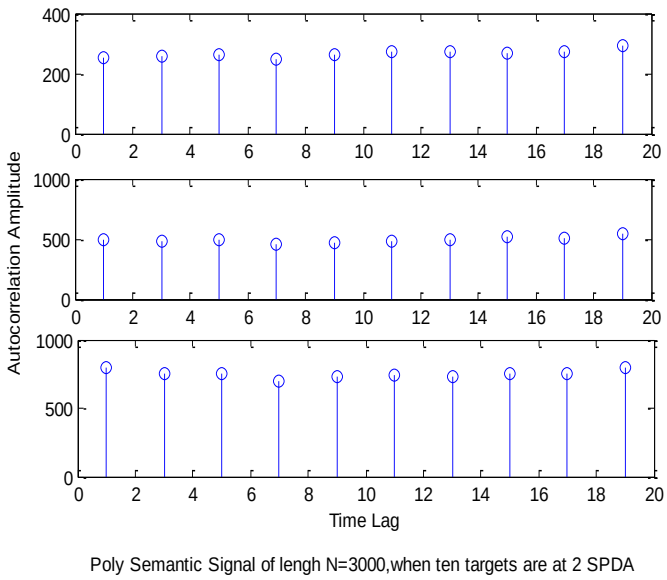

(a)

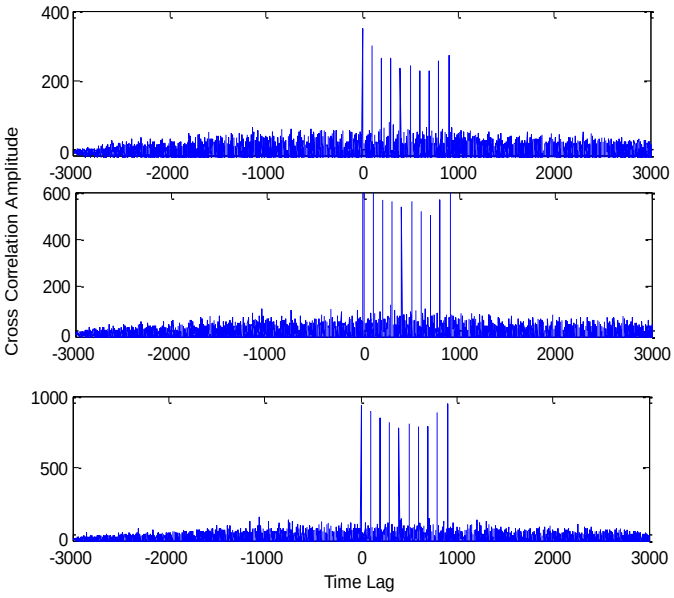

Poly Semantic Signal of lengh N=3000,when ten targets are at 100 SPDA

(b)

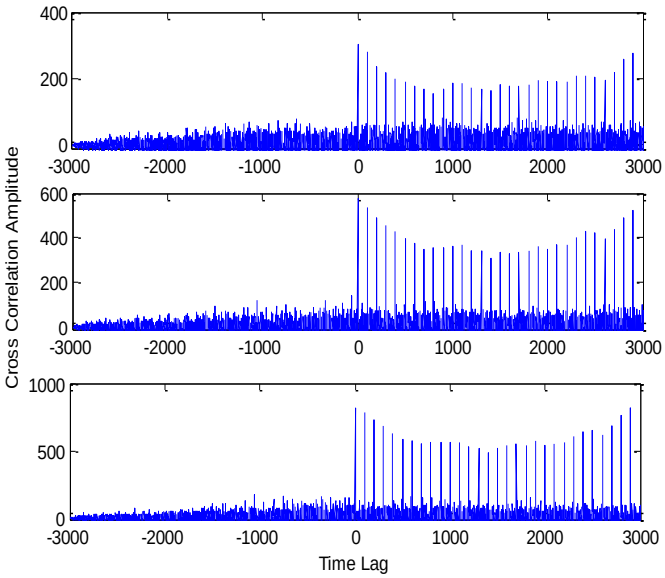

Poly Semantic Signal of lengh N=3000,when 30 targets are at 100 SPDA

(c)

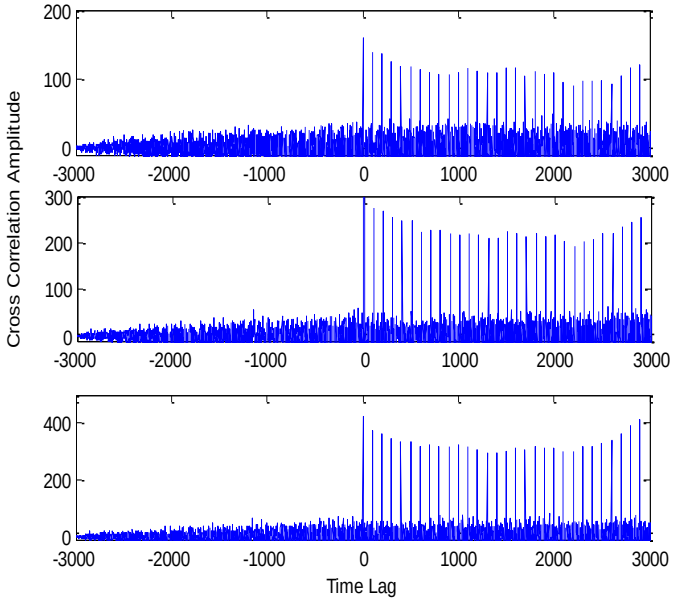

Poly Semantic Signal of lengh N=3000,when 30 targets are at 100 SPDA at -5dB noise

(d)

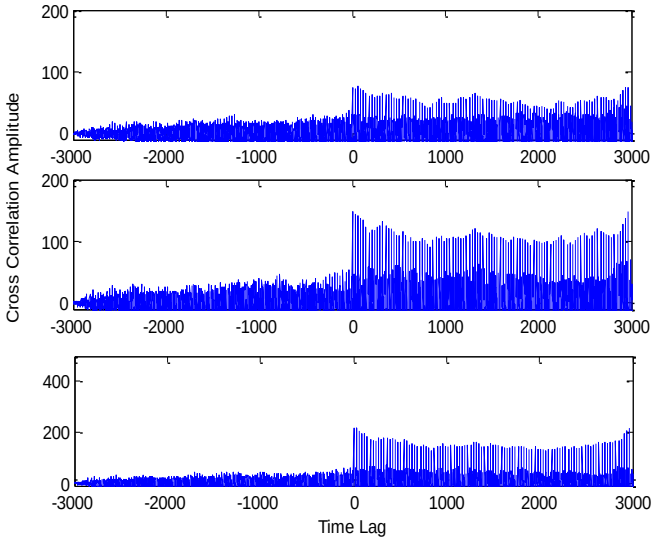

Poly Semantic Signal of lengh N=3000,when 100 targets are at 30 SPDA at noise -5dB

(e)

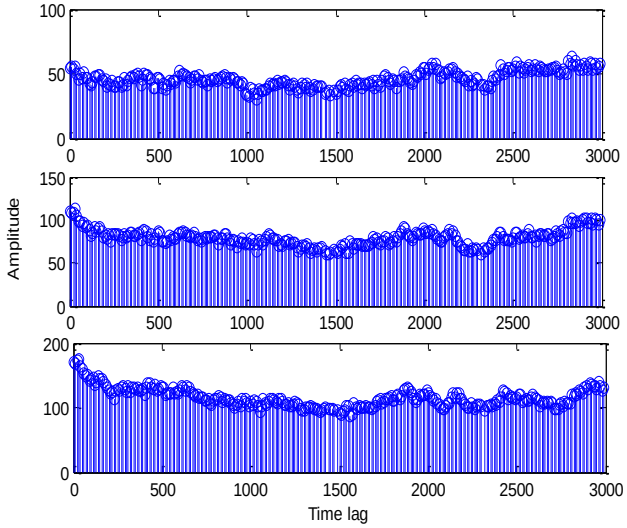

Poly Semantic Signal of lengh N=3000,when 300 targets are at 10 SPDA

(f)

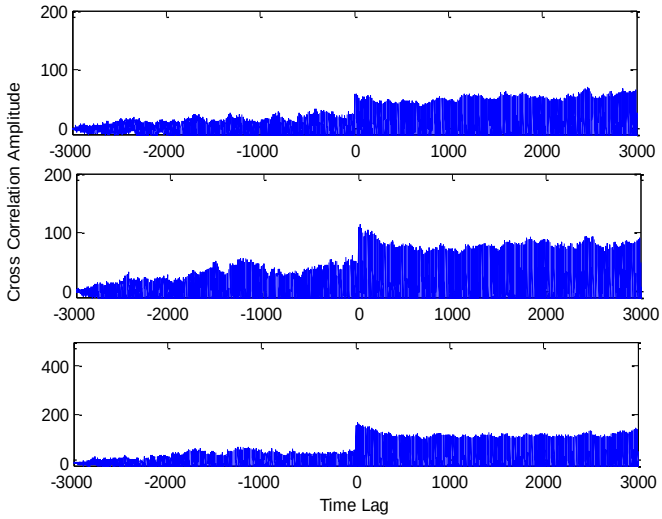

Poly Semantic Signal of lengh N=3000,when 300 targets are at 10 SPDA at -5dB Noise

(g)

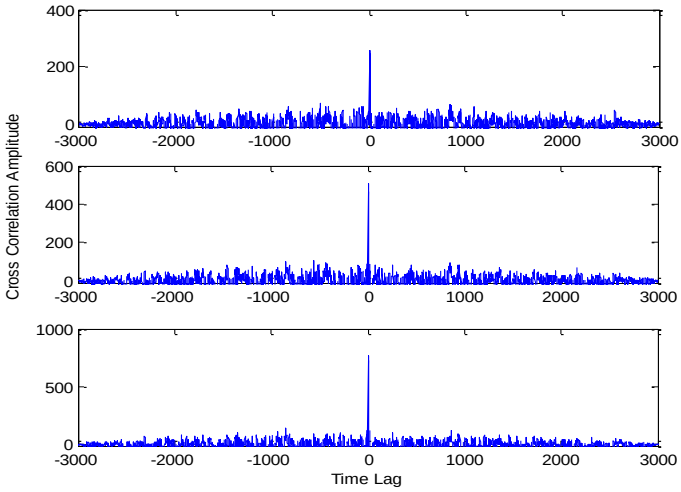

Poly Semantic Signal of lengh N=3000, for distributed target of duration 10 SPDA

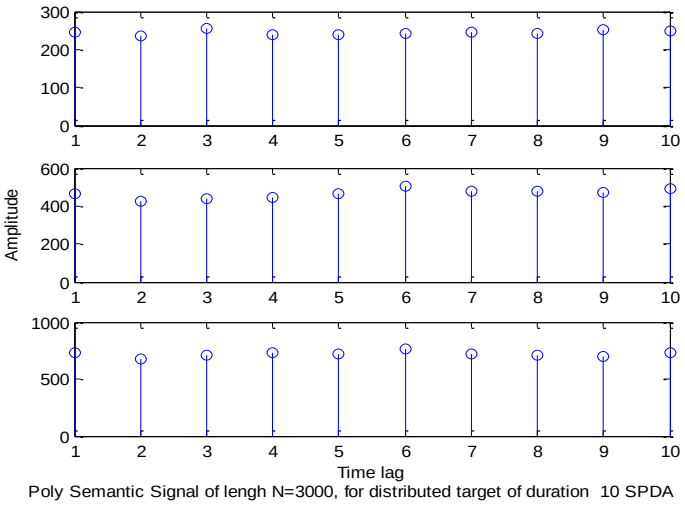

(h)

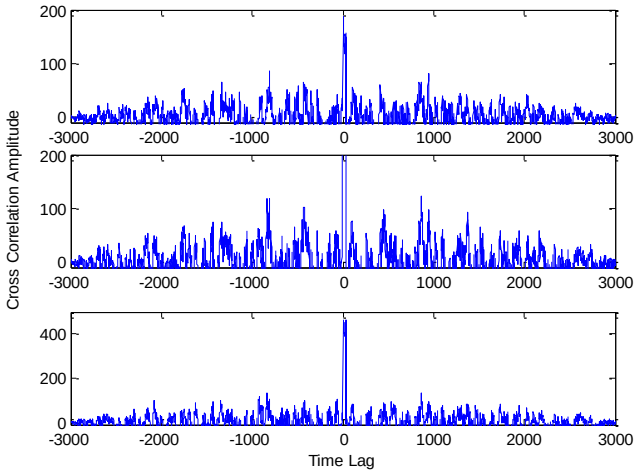

(i)

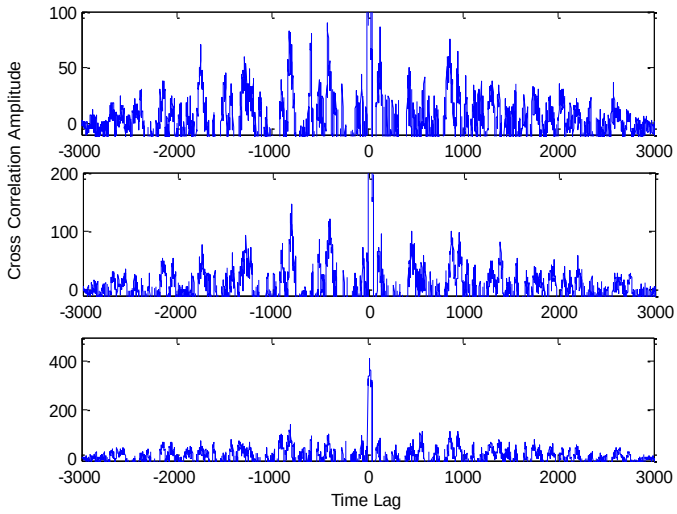

(j)

Fig. 13 Poly-semantic sequences of length 3000 for (a) 10 targets at 2 SPDA (b) ten targets at 100 SPDA (c) 30 targets at 100 SPDA (d) 30 targets at 100 SPDA at -5dB noise (e) 100 targets at 30 SPDA at -5dB noise (f) 300 targets at 10 SPDA (g) 300 targets at 10 SPDA at -5dB noise (h) distributed target of duration 10 SPDA (i) distributed target of duration 20 SPDA (j) distributed target of duration 50 SPDA

F. Ambiguity diagrams

Consider the following signal model for obtaining ambiguity diagrams [14], [15]. A Ka-band 30 GHz radar transmitting a Barker (B13) coded waveform with pulse interval of 650 ns and sub-pulse time interval 'τ 'of 50 ns (range resolution of 7.5m). The Doppler frequency ranges from -675 KHz to +675 KHz with maximum target radial velocity of 10 Mach (3375 m/s). To obtain the symmetry of the filter response on the ambiguity diagram, the zero Doppler frequency and the zero time lag are shifted to the center of the plot on x-y plane. Fig. 14 shows the ambiguity diagrams for poly-semantic sequences of length 1575, when two targets are at 500 SPDA (a) with no noise (b) and with SNR of -10dB.

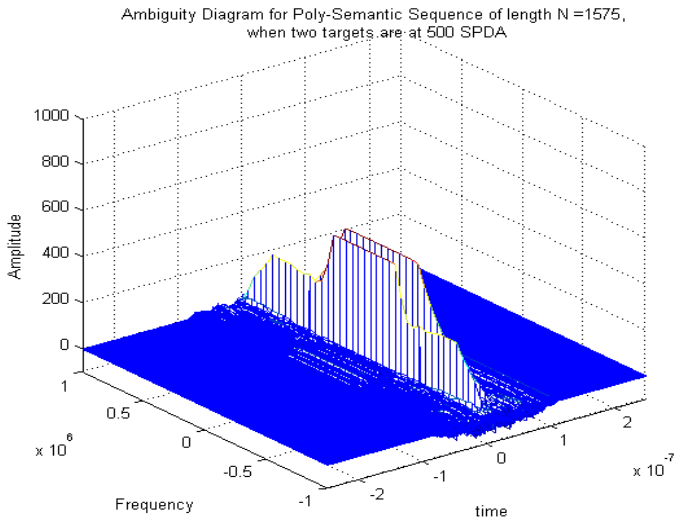

(a)

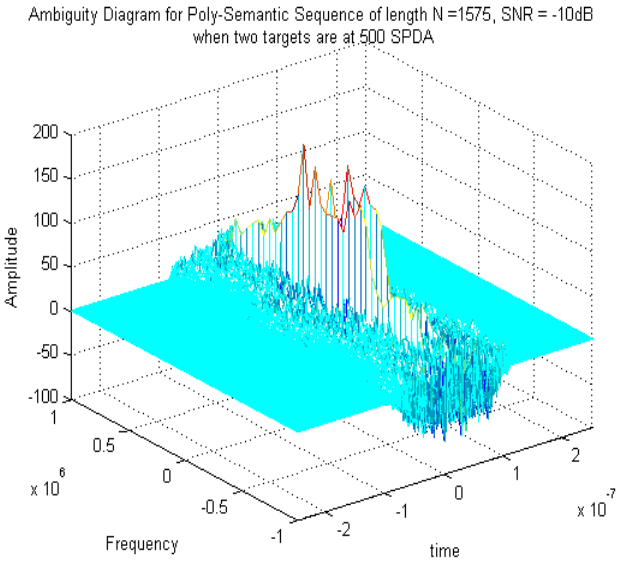

(b)

Fig. 14 shows the ambiguity diagram for poly-semantic sequences of length 1575, when two targets are at 500 SPDA (a) with no noise (b) with SNR of -10dB.

VI. CONCLUSIONS

In this paper poly-semantic sequences are analyzed for the detection of multiple target in high density additive noise and Doppler environment for the application of high resolution Doppler radar system. Table I shows that the PSS have higher figure of merit than any other poly alphabetic sequence in noise free environments particularly at larger sequence lengths. These results provide the evidence that the PSS with larger pulse compression ratios can achieve the range side lobe level below 14.78 dB. This is significance improvement over conventional pulse compression sequences [13] and poly-phase alphabetic sequences [6] which provide

side lobe level of 13.42 dB at length N > 1638 under noise free environment. This advantage arises because when the binary sequence is designed using 2nd order HBT algorithm, it performs recursive search such that the multiple interpretations of PSS of larger length reinforce each other through matched filtering and coincidence detection. The PSS has significant advantage of noise interference and Doppler tolerance with η below 20 dB at length N>4000. Another important advantage of PSS is that their detection ability is further improved in noise free or noisy environment through coincidence detection scheme. The poly-semantic sequences at higher lengths with coincidence detection has noise tolerance of η = -15dB. While compared with poly- phase sequences, a poly-semantic sequence has achieved better noise rejection ability, higher range resolution and superior Doppler tolerance. These examining results lead PSS to be very suitable for the high resolution Doppler radar systems. However, these advantages will be achieved with an additional affordable signal processing at the receiver.

REFERENCES

[1]. R. J. Keeler, C. A. Hwang, "Pulse compression for weather radar", in Proc. IEEE Int. Radar Conf., 1995, pp. 529-535.
[2]. F. B. Dah, C. F. Juang, and C. T. Lin, "A neural Fuzzy Network approach to Radar Pulse Compression", IEEE Trans. on geosciences and remote sensing letters., vol. 1, no. 1, 2004, pp. 15-20.
[3]. M. J. E. Golay, "The merit factor of long low autocorrelation binary sequences", IEEE Trans. Inf. Theory IT-28: 1982, 543-549.
[4]. P. Z. Peebles, J. R., "Radar Principles", John Wiley and Sons, Inc., 2004.
[5]. I. A. Pasha, N. Sudershan Rao, and P. S. Moharir, "Poly-alphabetic Pulse Compression Radar Signal Design", Modeling, Measurement & Control, Journal of AMSE, vol. 74, no. 4, 2001, pp. 57-64.
[6]. Y. Mallikarjuna Reddy, I. A. Pasha, and S. Vasthsal, "Poly-alphabetic radar signal processor for efficient target detection", International radar Symposium I, Bangalore, 2007, pp. 30-34.
[7]. I. A. Pasha, P. S. Moharir, and N. Sudarshan Rao, " Bi-alphabetic pulse compression radar signal design", Sadhana-Proc. Engg. Sci. Ind. Acad. Sci., vol. 25, 2000, pp. 481-488.
[8]. K. Deergha Rao and G. Sridhar, "Improving performance in pulse radar detection in using neural networks", IEEE Trans. Aerosp, Electron Sys, vol. 30, 1995, pp. 1193-1198.
[9]. H. K. Kawn and C. K. Lee, "Pulse radar detection using a multilayer neural network", Proc. Internat. Joint Conf. on Neural Networks,vol. 2, 1989, pp. 75-80.
[10]. H. K. kawn and C. K. lee, "A neural network approach to pulse radar detection", IEEE Trans.Aerospace Electron. Sys, vol. 29, 1993, pp. 9-21.
[11]. I. A. Pasha, P. S. Moharir, and V. M. Pandharipande, "Poly-semantic binary pulse compression radar sequences", IEEE TENCON 2003, IEEE technical conference on convergent technologies for the Asia-Pacific, 2003.
[12]. P. S. Moharir, K. RajaRajeswari, and K. Venkata Rao, "New figures of merit for pulse compression sequences", Journal of IETE, vol. 38, no. 4, 1992, pp. 209-216.
[13]. K. RajaRajeswari. *et al*, "New figures of merit for range resolution radar using hamming and Euclidean distance concepts", Proceedings of the 7th WSEAS International Conference on Multimedia Systems & Signal Processing, Hangzhou, China, April 15-17, 2007, pp. 139-145.
[14]. M. I. Skolnik, "Introduction to Radar Systems", Third Edition, McGraw Hill Inc., 1999.
[15]. A. W. Rihaczek, "Radar waveform selection: A simple approach", IEEE Trans. Aerospace Electron. Sys., vol. 7, 1971, pp1078-1086.